J|A|C|S
ARTICLES
Published on Web 12/09/2006

Population Balance Models and Monte Carlo Simulation for Nanoparticle Formation in Water-in-Oil Microemulsions: Implications for CdS Synthesis

Mani Ethayaraja and Rajdip Bandyopadhyaya*

Contribution from the Department of Chemical Engineering, Indian Institute of Technology Kanpur, Kanpur 208016, India

Received July 29, 2006; E-mail: rajdip@iitk.ac.in

Abstract: We address controlled CdS nanoparticle formation by tuning experimental synthesis conditions. To this end, a bivariate population balance equation (PBE) model has been developed based on time scale analysis, to explain the mechanism of nanoparticle formation in self-assembled templates. It addresses the process of mixing two water-in-oil (w/o) microemulsions, each containing a predissolved reactant in the microemulsion drops. Brownian collision and coalescence of two water drops of nanometer size results in mixing and exchange of reactant molecules, leading to chemical reaction. The water insoluble reaction product nucleates to form a nanoparticle in an individual drop, which subsequently grows internally by consuming the excess product and by coalescence-exchange with other drops. Finite rates of nucleation and coalescence-exchange are accounted for in the PBE, while the rates of reaction and internal growth of nanoparticles are found to be instantaneous. Experimentally proven binomial redistribution of reactant and product molecules upon drop coalescence is implemented in the present work. This results in a very good prediction of experimental data of the mean aggregate number (MAN) and hence size of CdS nanoparticles. Both our model and Monte Carlo (MC) simulation quantitatively capture the reported variation of MAN with molar excess of Cd^{2+} concentration and microemulsion drop size. Our results together with previous experimental data establish that usage of stoichiometrically five times or more of excess Cd^{2+} concentration can cause surface adsorption and desirable enhanced emission intensity of CdS nanoparticles, without altering particle size. We also propose a simplified and computationally efficient univariate PBE model. The univariate model gives very fast (in minutes) and accurate estimates (for low reactant concentrations) of the number and mean size of CdS nanoparticles. Time-scale analysis offers a good a priori choice of the appropriate model based on range of reactant concentrations.

1. Introduction

Nanoparticles of various materials have been synthesized in the liquid phase using self-assembled surfactant templates[1,2] and other techniques. Nanoparticle formation begins with energetically stable clusters, having a distinct magic number of monomer units. For example, CdS crystallizes in the form of $(CdS)_{13}$, $(CdS)_{16}$, $(CdS)_{33}$, $(CdS)_{34}$, $(CdS)_{57}$, $(CdS)_{81}$, and so forth.[3,4] Various analytical techniques (powder X-ray diffraction, UV−vis spectroscopy, mass spectrometry, etc.) and ab initio calculations suggest that these clusters crystallize in cage-like forms, similar to the case of fullerenes.[3] Molecular simulations have been carried out to identify energetically favored structures for these clusters. This is done in a way so as to fit the calculated electronic properties (based on these structures), with experimental property data.[5] Subsequently, the clusters grow in solution and form nanoparticles, having crystalline structures similar to those of bulk crystals.[6]

A recent molecular simulation study showed the very early stages (time scale of nanoseconds) of nucleation of stable ZnS clusters from an aqueous solution.[7] Together, these simulation studies are concerned with the formation of clusters from their monomer units[7] and cluster structure−property correlations.[5] However, from these studies, it is not known how the monomer is formed by reaction in a typical synthesis method and how the clusters grow in solution by consuming monomers to form the final nanoparticles. Therefore, it will be very important to have a model which correlates various experimental conditions to the formation of clusters, and their growth, by accounting for a sequence of processes like reaction, nucleation, and growth of nanoparticles. Hence, we would like to develop a model to predict mean nanoparticle size and size distribution, which, on combining with previous molecular modeling studies for clusters, will give the complete means of tuning experimental synthesis conditions to desired electronic and optical properties

(1) Pileni, M. P. *Langmuir* **1997**, *13*, 3266.
(2) Holmberg, K. *J. Colloid Interface Sci.* **2004**, *274*, 355.
(3) Kasuya, et al. *Nat. Mater.* **2004**, *3*, 99.
(4) Joswig, J.-O.; Springborg, M.; Seifert, G. *J. Phys. Chem. B* **2000**, *104*, 2617.
(5) Jose, R.; Zhanpeisov, N. U.; Fukumura, H.; Baba, Y.; Ishikawa, M. *J. Am. Chem. Soc.* **2006**, *128*, 629.
(6) Talapin, D. V.; Rogach, A. L.; Kornowski, A.; Haase, M.; Weller, H. *Nano Lett.* **2001**, *1*, 207.
(7) Hamad, S.; Cristol, S.; Catlow, C. R. *J. Am. Chem. Soc.* **2005**, *127*, 2580.

10.1021/ja0652621 CCC: $33.50

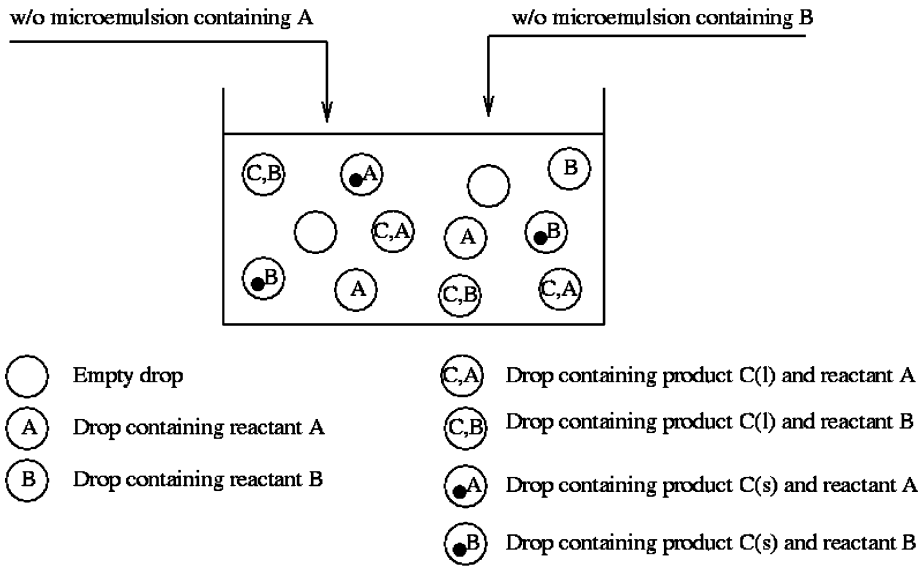

Figure 1. Schematic of the method of mixing and reaction of two microemulsions for synthesizing nanoparticles.

of CdS nanoparticles. Thus, the present work can bridge the knowledge of nanoparticle formation to their properties.

Furthermore, previous simulations predict only a single cluster or nanoparticle size. However, the present model should be able to capture the formation of clusters of various sizes and their dissimilar growth rates, leading to information about the complete size distributions, seen experimentally. Finally, we aim to develop computationally more efficient models, compared to time-consuming molecular simulation studies.

One of the widely studied liquid-phase templates is a water-in-oil (w/o) microemulsion solution, which consists of surfactant stabilized water drops of nanometer size, dispersed in an oil medium. In this paper, we are concerned with only self-assembled templates and will use the term *drop* to denote a spherical water drop of a w/o microemulsion system. Reactants necessary for nanoparticle formation are introduced into the drops, either by external mass transport or by mixing two microemulsions having predissolved reactants. The drops collide with each other due to Brownian motion and occasionally coalesce by opening of their surfactant layers.[8,9] The resulting coalesced form of two drops is called a dimer, which has a very short life time ($\approx 25\ \mu$s).[10] In the dimer, the contents of the drops are well mixed due to their small size whereupon reaction takes place. Subsequently, the dimer redisperses into two equal sized daughter drops into which the reactant and product molecules of the dimer are redistributed. The insoluble reaction product then nucleates to form a solid particle, which grows inside the drop. Importantly, reaction, redispersion, nucleation, and growth are confined within the drops. As a result, size controlled nanoparticles can be formed by easily changing drop size, which is a further motivation of the present study.

Therefore, we focus on developing a mathematical model for microemulsion mediated synthesis of nanoparticles in this paper. It should predict the mean aggregate number (MAN), a measure of nanoparticle size, and the complete size distribution as a function of various process variables, like drop size, reactant concentration, and molar ratio of reactants.

2. Background on Microemulsion Mediated Nanoparticle Modeling

There are various methods of nanoparticle synthesis using w/o microemulsions, which differ from one another in the way reactants are introduced into the drops. These methods can be broadly classified into two types, employing either one or two microemulsion solutions. In the first type, one of the reactants is predissolved in the drops and another reactant (in liquid or gaseous form) is added directly into the microemulsion solution. The latter diffuses into the drops through the continuous oil medium and reacts with the predissolved reactant. For example, $CaCO_3$ nanoparticles were produced by sparging CO_2 gas into a w/o microemulsion solution, which contained a predissolved $Ca(OH)_2$ solution.[11] The second method, in contrast, employs two microemulsion solutions, each one having a predissolved reactant. The two solutions are then mixed, whence coalescence-exchange of drops brings the two reactants together in the dimer (Figure 1). This forms an important and often the only synthesis route to some nanoparticles. Materials like silver halides,[12,13] metal sulfides,[14−17] metals,[18−20] etc. were among many others synthesized by this method.

Irrespective of the route followed, nanoparticle formation involves reaction inside the drops, followed by particle nucleation and growth. Nevertheless, coalescence-exchange of drops continuously changes the distribution of molecules in drops, thus affecting all the elementary processes, which in addition occur simultaneously.

(8) Eicke, H. -F.; Shepherd, J. C. W.; Steinemann, A. *J. Colloid Interface Sci.* **1976**, *56*, 168.
(9) Robinson, B. R.; Steytler, D. C; Tack, R. D. *J. Chem. Soc., Faraday Trans. 1* **1979**, *75*, 481.
(10) Fletcher, P. D. I.; Howe, A. M.; Robinson, B. H. *J. Chem. Soc., Faraday Trans. 1* **1987**, *83*, 985.
(11) Kandori, K.; Kon-No, K.; Kitahara, A. *J. Colloid Interface Sci.* **1988**, *122*, 78
(12) Monnoyer, Ph.; Fonseca, A.; Nagy, J. B. *Colloids Surf., A* **1995**, *100*, 233.
(13) Sato, H.; Hirai, T.; Komasawa, I. *J. Chem. Eng. Jpn.* **1996**, *29*, 501.
(14) Lianos, P.; Thomas, J. K. *Chem. Phys. Lett.* **1986**, *125*, 299.
(15) Lianos, P.; Thomas, J. K. *J. Colloid Interface Sci.* **1986**, *117*, 505.
(16) Hirai, T.; Sato, H.; Komasawa, I. *Ind. Eng. Chem. Res.* **1994**, *33*, 3262.
(17) Hirai, T.; Tsubaki, Y.; Sato, H.; Komasawa, I. *J. Chem. Eng. Jpn.* **1995**, *28*, 468.
(18) Chen, D. H.; Wang, C. C.; Huang, T. C. *J. Colloid Interface Sci.* **1999**, *210*, 123.
(19) Chiang, C. L. *J. Colloid Interface Sci.* **2000**, *230*, 60.
(20) Ingelsten, H. H.; Bagwe, R.; Palmqvist, A.; Skoglundh, M.; Svanberg, C.; Holmberg, K.; Shah, D. O. *J. Colloid Interface Sci.* **2001**, *241*, 104.

It is, hence, essential for a model of nanoparticle formation to include both the correct redistribution mechanism of reactant and product molecules during coalescence-exchange and use validated kinetic rate expressions for elementary processes. Natarajan et al.[21] accounted for a finite rate of only coalescence-exchange in their population balance equation (PBE) model for the single microemulsion method, with the assumption that all the other processes are instantaneous. They used the unrealistic cooperative redistribution mode for redistribution of molecules. Bandyopadhyaya et al.[22,23] and Ethayaraja et al.[24] modeled the single microemulsion problem accounting for both finite rates for nucleation and coalescence-exchange. Nucleation rate in each drop was calculated individually by considering the statistical distribution of molecules over the drops. Based on time-scale analysis, they showed reaction and growth are instantaneous in comparison and classified all the drops into only two kinds: drops with or without a nanoparticle. PBEs and their moment transformation were written for both these populations, and they successfully predicted average particle size and variance of nanoparticles obtained in experiments.

The models described above for a single microemulsion method were based on univariate PBEs, because drops were identified by a single state variable, namely, the number of product molecules in each drop. This was possible because the rate of coalescence-exchange of drops was faster than the rate of addition of an external gaseous or liquid reactant (A). Thus as long as reactant B was present in the system, reactant A molecules which diffused into the drops could redistribute very fast by coalescence-exchange with some other drops, wherein it reacted with B. Therefore, each drop was characterized by only the product molecules, leading to the univariate PBE model. However, in case of the other route of mixing two microemulsion solutions, both the reactants are present in the mixed solution to start with itself (but in different drops). Therefore, as coalescence-exchange brings the two reactants together, it is necessary to account for the evolving distribution of both reactant and product molecules in drops as a function of time. Thus, modeling this synthesis route would require multivariate PBEs. To this end, Kumar et al.[25] have recently reported a comprehensive bivariate PBE model for a system of two reacting microemulsions. They considered drops of seven classes, with finite rates of coalescence-exchange and nucleation. Assuming reaction and growth are instantaneous, drops were identified by two variables: number of one of the reactant and product molecules. They, therefore, extended the univariate model of Bandyopadhyaya et al.[22,23] developed for a single microemulsion system to a bivariate model for a system of two microemulsions. However, Kumar et al.[25] used the simple but unrealistic cooperative redistribution in coalescence-exchange of drops. So their prediction of experimental data was merely qualitative.

In general, the minimum number of variables needed to classify drop populations can be decided by time scale analysis of all the elementary events in nanoparticle formation. It may then be necessary to write PBEs with more than two variables. For example, when the rates of reaction and growth of nanoparticles are comparable to nucleation and coalescence-exchange, then four variables (both the predissolved reactants and product in liquid and solid form) are required to define the state of each drop. If one of these two rates is instantaneous, three variables are sufficient. However, PBE models with three or more state variables become complicated and difficult to derive due to combinatorial complexity. It is in this context that parallel efforts in Monte Carlo (MC) simulation are useful. At the cost of large computational times, MC simulation can handle any number of state variables and also incorporate a complex functional dependence of rate or redistribution modes on various system parameters. Indeed MC simulation has been carried out to simulate nanoparticle size distribution.[26−31] Bivariate PBE models as well as MC simulation have been used in other areas of particulate processing as well, for example, for describing coagulation and sintering behavior of particles in a flame reactor[32] or for kinetics of emulsion drops in extraction involving liquid emulsion membranes.[33]

Redistribution of molecules, in principle, can be binomial or cooperative in nature. It is well-established that the kinetics of coalescence-exchange of molecules in w/o microemulsion systems follows the binomial redistribution mode.[34−36] Hatton et al.[37] derived univariate PBEs using various redistribution modes to interpret exchange kinetics of water drops from their model. However, they did not use this information to model nanoparticle formation.

The aim of this paper is, therefore, to develop a general bivariate PBE model to quantitavely describe nanoparticle synthesis on reacting two w/o microemulsion solutions. It should incorporate a correct description of events with finite rates, with an accurate redistribution mode (binomial) for the exchange of molecules. The model results will be compared with the experiments of Lianos and Thomas[14] and both new and previously published[27] MC simulation results. The PBE model and MC simulation together will give further insight into the role of various operating variables on mean nanoparticle size and complete size distribution. Further analysis will also be done to derive a computationally efficient univariate model and examine the regime of experimental conditions in which it is applicable. Thus, one would be able to review the need and use of univariate and bivariate PBE models for predicting the nanoparticle synthesis process.

3. Population Balance Models

We have developed a general model that can be extended or modified to explain various methods of producing nanoparticles using w/o microemulsions or other forms of self-assembled templates, as appropriate. In particular, we focus on the method

(21) Natarajan, U.; Handique, K.; Mehra, A.; Bellare, J. R.; Khilar, K. *Langmuir* **1996**, *12*, 2670.
(22) Bandyopadhyaya, R.; Kumar, R.; Gandhi, K. S.; Ramkrishna, D. *Langmuir* **1997**, *13*, 3610.
(23) Bandyopadhyaya, R.; Kumar, R.; Gandhi, K. S. *Langmuir* **2001**, *17*, 1015.
(24) Ethayaraja, M.; Dutta, K.; Bandyopadhyaya, R. *J. Phys. Chem. B* **2006**, *110*, 16471.
(25) Kumar, A. R.; Hota, G.; Mehra, A.; Khilar, K. C. *AIChE J.* **2004**, *50*, 1556.
(26) Li, Y.; Park, C.-W. *Langmuir*, **1999**, *15*, 952.
(27) Bandyopadhyaya, R.; Kumar, R.; Gandhi, K. S. *Langmuir* **2000**, *16*, 7139.
(28) Singh, R.; Durairaj, M. R.; Kumar, S. *Langmuir* **2003**, *19*, 6317.
(29) Voigt, A.; Adityawarman, D.; Sundmacher, K. *Nanotechnol.* **2005**, *16*, s429.
(30) Jain, R.; Mehra, A. *Langmuir* **2004**, *20*, 6507.
(31) Shukla, D.; Mehra, A. *Nanotechnol.* **2006**, *17*, 261.
(32) Wright, D. L.; McGraw, R.; Rosner, D. E. *J. Colloid Interface Sci.* **2001**, *236*, 242.
(33) Bandyopadhyaya, R.; Bhowal, A.; Datta, S.; Sanyal, S. K. *Chem. Eng. Sci.* **1998**, *53*, 2799.
(34) Tachiya, M. *Can. J. Phys.* **1990**, *68*, 979.
(35) Bommarius, A. S.; Holzwarth, J. F.; Wang, D. I. C.; Hatton, T. A. *J. Phys. Chem.* **1990**, *94*, 7232.
(36) Infelta, P. P.; Graglia, R.; Minero, C.; Pelizzetti, E. *Colloids Surf.* **1987**, *28*, 289.
(37) Hatton, T. A.; Bommarius, A. S.; Holzwarth, J. F. *Langmuir* **1993**, *9*, 1241.

of mixing two reactive microemulsions, which necessitates multivariate PBEs. The mechanism is shown as follows:

$$A + B \xrightarrow{\text{reaction}} C\,(l) \xrightarrow{\text{nucleation}} C\,(s)\downarrow$$

A single drop may have all the four components [A, B, C(l), and C(s)] coexisting together, which necessitates four state variables for each drop. However, if reaction of A and B and growth of C(s) by consumption of C(l) are instantaneous, then only two variables are sufficient. In the following, justification of this possibility leading to bivariate PBE is discussed based on time-scale analysis.

3.1. Time-Scale Calculations and Analysis. 1. In general, precipitation reactions are extremely fast and can be treated as instantaneous.[22,23,38] For the specific case of CdS, this time scale (τ_r) is of the order of 10^{-8} s.[39] Compared to the lifetime of a dimer ($\tau_d \sim 10^{-5}$ s),[10] reaction is hence instantaneous. This implies that reaction is completed in the dimer itself, and only product molecules [C(l)] and excess reactant molecules (either A or B) are to be redistributed in daughter drops. So reactants A and B will not coexist in a drop.

2. The time scale of growth of the C(s) nanoparticle by consuming a liquid C(l) molecule in a drop (τ_g) calculated[39] using the Smoluchowski[40] equation is of the order of 10^{-10} s.[23]

3. Nucleation rate is calculated using classical nucleation theory for homogeneous nucleation. In a drop having i number of C(l) molecules, the nucleation rate is given by[23]

$$k_n(i,t) = 0 \qquad \text{for } i < n^*$$

$$= ik_0 \exp\left(\frac{-16\pi\sigma^3 v_m^{\,2}}{3(k_B T)^3[\ln(\lambda(t))]^2}\right) \quad \text{for } i \geq n^* \tag{1}$$

where σ is the interfacial tension between solid nuclei and surrounding drop liquid, v_m is the volume of one C(s) molecule, λ is the supersaturation ratio of C(l), and n^* is the critical number of C molecules in a nucleus. The time scale of nucleation (τ_n) is calculated from the inverse of $k_n(n^*)$. For CdS particle nucleation, τ_n is of the order of 10^{-3} s.

Therefore, growth of the existing nanoparticle in a drop by consumption of liquid C(l) molecules is instantaneous compared to the rate of formation of a second nucleus in the same drop. So C(s) and C(l) do not coexist in a drop. Therefore, a drop can have only one particle at the most, with or without one of the reactants (either A or B) in addition.

4. The rate of collision (q_d) of two spherical drops of volume v_1 and v_2 is given by Smoluchowski equation[40] as

$$q_d = \frac{2k_B T}{3\eta}\left[2 + \left(\frac{v_1}{v_2}\right)^{1/3} + \left(\frac{v_2}{v_1}\right)^{1/3}\right] \tag{2}$$

For equal sized drops, eq 2 reduces to

$$q_d = \frac{8k_B T}{3\eta} \tag{3}$$

For two classes of drops with number densities (number per unit volume of microemulsion) n_1 and n_2, the rate of coalescence is given by $\beta_d q_d n_1 n_2$. β_d is the coalescence efficiency of drop−drop collisions. For a number density of 10^{18} cm^{-3} of drops, the time scale of coalescence-exchange of drops ($\tau_c = 1/\beta_d q_d N_{drop}$) is of the order of 10^{-3} s. Therefore, coalescence-exchange of drops and nucleation proceed at finite and comparable rates. Conclusions from the above time scale analysis are summarized in Table 1.

Table 1. Time-Scale Analysis and Conclusions

time-scale comparison	conclusions
$\tau_r < \tau_d$	• instantaneous reaction of A and B • reactants A and B do not coexist in a drop
$\tau_g \ll \tau_n(n^*)$	• instantaneous growth of C(s) particle • C(s) and C(l) do not coexist in a drop • either none or one C(s) particle in a drop
$\tau_c \approx \tau_n(n^*)$	• coalescence-exchange and nucleation rates are comparable to each other and rate controlling

Table 2. Classification of Drops for the Bivariate PBE Model

class of drop	description: (number density of drops having)
$n_A(i)$	i molecules reactant A
$n_B(i)$	i molecules reactant B
$n_{CA}(i,j)$	i molecules of C(l) and j molecules of reactant A
$n_{CB}(i,j)$	i molecules of C(l) and j molecules of reactant B
$n_{SA}(i,j)$	i molecules of C(s) and j molecules of reactant A
$n_{SB}(i,j)$	i molecules of C(s) and j molecules of reactant B
$n(0)$	empty drops; none of A, B, C(l), or C(s)

Before mixing, the individual microemulsion solutions have only two classes of drops: empty and those having a finite number of either A or B reactant molecules. After mixing, coalescence-exchange of drops introduces new classes of drops in the system due to reaction, nucleation, and growth. Based on previous assumptions, the population of drops could be classified into seven classes as shown in Table 2, similar to that of Kumar et al.[25] The drops, characterized either by a single or two state variable indices, are referred to as univariate and bivariate classes of drops, respectively. The state variables are the number of molecules, which is a discrete number. This is due to a very low occupancy of the number of molecules in a drop. Therefore, the resulting PBE itself is discrete and obviates the need for any further discretization, whereas continuous PBEs have to be discretized for numerical solutions.[32]

3.2. Rules of Coalescence-Exchange. For bivariate drops, each type of molecule is redistributed independent of the other. The possible collision and binomial redistribution schemes are summarized below.

1. Consider coalescence between two univariate drops from the same class (n_A and n_A or n_B and n_B) or between univariate and empty drops [n_A and $n(0)$ or n_B and $n(0)$]. For example, if $n_A(j)$ and $n_A(k)$ coalesce (Figure 2a), the expectation that one of the daughter drops would get i out of $(j + k)$ molecules is given by

$$E(i, j+k) = p_{i,j+k} + p_{j+k-i,j+k} \tag{4}$$

where,

$$p_{i,j+k} = \frac{(j+k)!}{i!(j+k-i)!}\left(\frac{1}{2}\right)^{j+k} \tag{5}$$

(38) Rauscher, F.; Veit, P.; Sundmacher, K. *Colloids Surf. A.* **2005**, *254*, 183.
(39) Towey, T. F.; Khan-Lodhi, A.; Robinson, B. H. *J. Chem. Soc., Faraday Trans.* **1990**, *86*, 3757.
(40) Smoluchowski, M. V. *Phys. Z.* **1916**, *17*, 557.

Therefore the other drop gets $(j + k - i)$ molecules. Since the drops are indistinguishable in this case, these two probabilities should be same.

Hence,

$$E(i, j + k) = 2\, p_{i,j+k} \tag{6}$$

2. Consider a drop containing a solid particle and any one type of reactant molecules (n_{SA} or n_{SB}), coalescing with a univariate drop having the same kind of reactant (n_A or n_B, respectively). In this case the drops are distinguishable, because the particle is retained in the original drop. For example, when $n_A(l)$ and $n_{SA}(j,k)$ coalesce (Figure 2b), the expectation that a daughter drop would get i number of A molecules out of $(k + l)$ is given by

$$\tilde{E}(i, k + l) = p_{i,k+l} \tag{7}$$

3. When two same classes of drops each having a particle in them (n_{SA} and n_{SA} or n_{SB} and n_{SB}) coalesce (Figure 2c), the particles are retained in the respective parent drops. Only the total reactant molecules are redistributed according to rule 2, since the drops are distinguishable.

4. During coalescence of drops having opposite kinds of reactants, a dimer could be formed with two kinds of molecules [C(l) and the excess reactant in these two drops] in it. This situation can occur due to coalescence of many different classes of drops. For example, coalescence between $n_A(k)$ and $n_B(l)$, with $k > l$, would form a dimer with l number of C(l) and $(k - l)$ number of reactant A molecules (Figure 2d). Therefore, if a dimer has l molecules of type 1 and k molecules of type 2, then the expectation for a drop to get i molecules of type 1 and j molecules of type 2 on redistribution is given by

$$E(i, l; j, k) = p_{i,l}\, p_{j,k} + p_{l-i,l}\, p_{k-j,k} \tag{8}$$

Since drops are indistinguishable,

$$E(i,l; j,k) = 2p_{i,l}\, p_{j,k} \tag{9}$$

5. For coalescence (Figure 2f) between drops, which contain a particle and different kinds of reactants (n_{SA} and n_{SB}) between themselves, both newly formed reaction product C(l) and the excess reactant are redistributed independently between the daughter drops. The particles grow instantaneously by consuming the redistributed C(l) available to each drop. Therefore, for a dimer containing two particles, k number of C(l) and l number of reactant A (or B) molecules, the expectation for a daughter drop to get i number of C(l) and j number of reactant A (or B) is

$$\tilde{E}(i,k; j,l) = p_{i,k}\, p_{j,l} \tag{10}$$

6. Figure 2e shows the nucleation process of a drop supersaturated with C(l) molecules. Thus $n_{CA}(i,j)$ nucleates when $i \geq n^*$.

3.3. Bivariate Population Balance Model. Population balance equations are conservation equations for the number densities of different classes of drops. With the aforementioned rules and finite rates of coalescence-exchange and nucleation, the PBE for number density of bivariate classes of drops is written as

$$\frac{dn_k(i, j, t)}{dt} = B_k(t) - D_k(t) \qquad \text{for } k = \text{CA, CB, SA, SB} \tag{11}$$

For univariate drop classes (k = A, B), $n_k(i, t)$ is used in the above equation. B_k and D_k are birth and death rates of k^{th} class of drops due to coalescence-exchange and nucleation. For example, the birth of a member of a particular class of drop can be due to many different coalescence-exchange events having finite probabilities to form this member. Conversely, a single coalescence-exchange event can contribute as death terms for two different classes of drops. As the total number of drops is conserved, the number density of empty drops is calculated by subtracting the sum of number densities of all other classes from the initial total number density. Similarly nucleation of a particle contributes as a death term in the CA or CB population balance equation and simultaneously as a birth term in the SA or SB population balance, respectively.

The number densities of all classes of drops are nondimensionalized with respect to the total number density of drops as follows,

$$\bar{n}_k(i, t) = \frac{n_k(i, t)}{N_{drop}} \tag{12}$$

The complete form of PBEs considering binomial redistribution (eq 11) is given in Appendix A (see Supporting Information). These equations can be suitably modified for cooperative redistribution.

3.4. Univariate Population Balance Model. In some cases, especially at low reactant concentrations, the mean numbers of A and B reactant molecules per drop (μ_A, μ_B) are both less than 1. Under this condition, both the number densities of bivariate drops and the rate of change of their number densities are very low. So compared to univariate drops, contribution of bivariate drops to the evolution of the nanoparticle size distribution is not significant. This can be justified by a time-scale analysis of the formation of bivariate drops as follows.

We use the Poisson distribution of both A and B reactant molecules in the drops at time $t = 0$. Bivariate drops are more likely to appear when any drop having two or more reactant molecules of either kind (A or B) coalesce with another nonempty drop. Coalescence-exchange among $n(0)$, $n_A(1)$, and $n_B(1)$ class of drops (Table 3) results in the formation of univariate drops, the latter containing either reactant or product molecules. In general, time scale of coalescence-exchange events of drops having i number of reactant molecules is given by $1/[\beta_d q_d n(i)]$. Therefore, the time scale of formation of the bivariate population is given by

$$\tau_b = \frac{1}{\beta_d q_d \left(\sum_{i=2}^{\infty} [n_A(i) + n_B(i)]\right)} \tag{13}$$

Noting that

$$n(0) + \sum_{i=1}^{\infty} [n_A(i) + n_B(i)] = N_{drop} \tag{14}$$

and nondimensionalizing individual number densities with N_{drop},

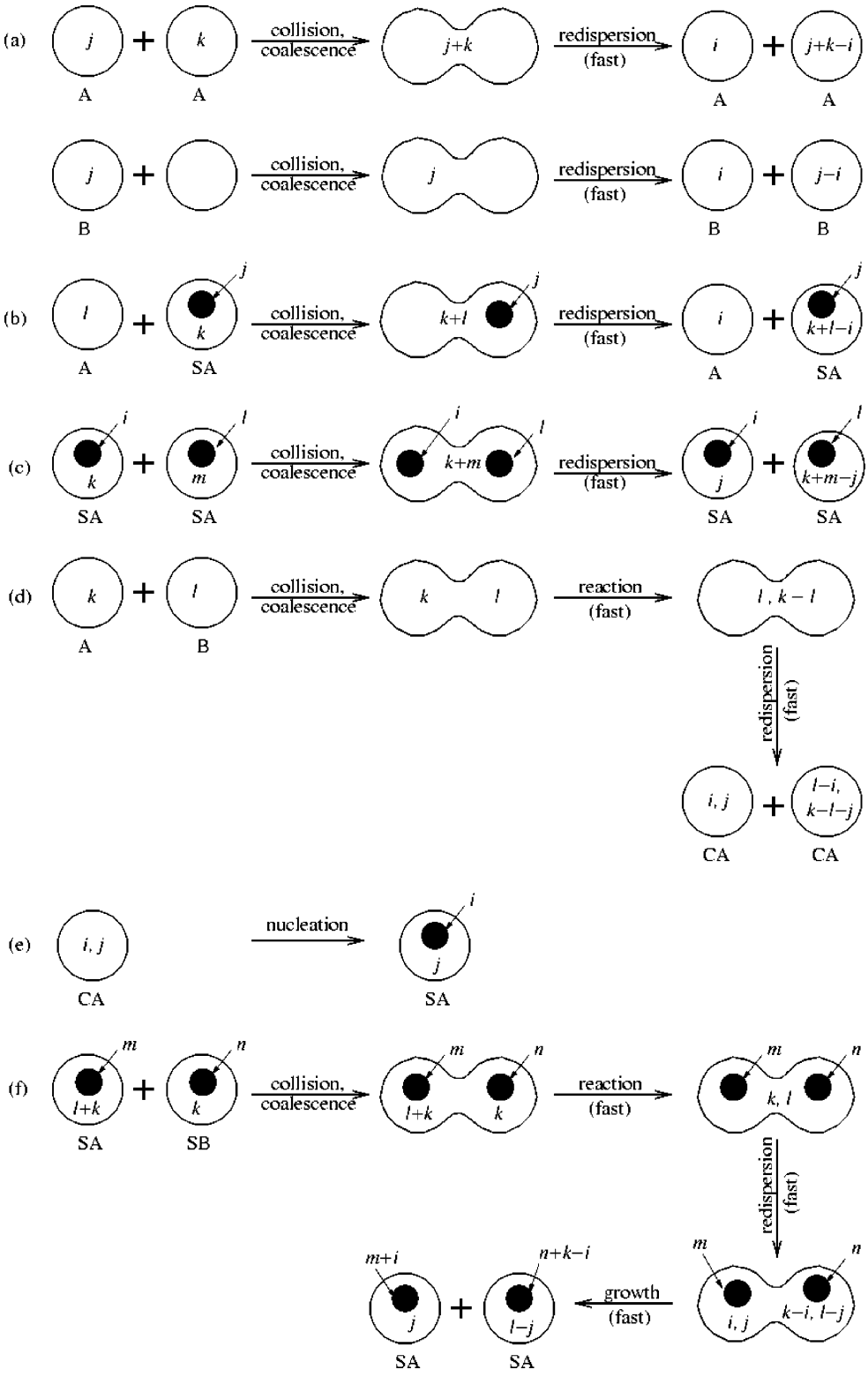

Figure 2. Coalescence-exchange of drops involving univariate and bivariate distributions.

from eq 13 we have

$$\tau_b = \frac{1}{\beta_d q_d N_{drop}[1 - \bar{n}(0) - \bar{n}_A(1) - \bar{n}_B(1)]} \qquad (15)$$

Using the initial distribution of reactant molecules to be Poisson, from eq 15,

$$\tau_b = \frac{1}{\beta_d q_d N_{drop}\left(1 - \frac{1}{2}e^{-\mu_A}(1+\mu_A) - \frac{1}{2}e^{-\mu_B}(1+\mu_B)\right)} \qquad (16)$$

Nondimensionalizing τ_b with the total coalescence time scale

Table 3. Classification of Drops for the Univariate PBE Model

class of drop	description: (number density of drops having)
$n_A(i)$	i molecules of reactant A
$n_B(i)$	i molecules of reactant B
$n_C(i)$	i molecules of C(l)
$n_S(i)$	i molecules of C(s)
$n(0)$	empty drops; none of A, B, C(l), or C(s)

involving drops of all kinds [$\tau_c = 1/(\beta_d q_d N_{drop})$], we get

$$\bar{\tau}_b = \frac{1}{\left(1 - \frac{1}{2}e^{-\mu_A}(1+\mu_A) - \frac{1}{2}e^{-\mu_B}(1+\mu_B)\right)} \quad (17)$$

For the special case of $\mu_A = \mu_B = \mu$, eq 17 becomes

$$\bar{\tau}_b = \frac{1}{[1 - e^{-\mu}(1+\mu)]} \quad (18)$$

Therefore, when μ is small, $\bar{\tau}_b$ is high, and bivariate drops form very slowly. Number densities of bivariate drops then remain negligibly small, and the univariate model can be fairly satisfactory. From Table 4, for $\mu = 0.1$, the rate of formation of bivariate drops is two orders of magnitude slower than that of univariate drops, making the former negligible. This conclusion is true even for $\mu = 0.5$. However, as μ becomes 1, bivariate drops form almost at the same time scale as that of univariate drops, so that the bivariate population becomes non-negligible. For $\mu = 2$, the bivariate population is certainly important, as both classes of drops form with similar time scales.

Based on this pseudo steady state approximation then, it is sufficient to consider only the univariate drop populations, under certain conditions. Therefore, a univariate PBE model (derived from the bivariate model of section 3.3) can be used without loss of much accuracy. So we define a total of five univariate drop classes (Table 3), compared to seven drop classes for the bivariate model (Table 2). PBEs for the univariate model are written (Appendix B, see Supporting Information) neglecting all the coalescence events that would result in the generation of bivariate populations. The coalescence-exchange rules defined for the bivariate model also apply to the univariate PBE model.

3.5. Initial Conditions and Solution Methodology. It is known that coalescence-exchange with binomial redistribution gives rise to Poisson distribution in the number of reactant molecules per drop at steady state.[36] So the initial reactant distribution in drops of each microemulsion, before mixing, is calculated from Poisson distribution as follows:

$$n_A^0(i) = N_{drop,A}\frac{e^{-\mu_A}\mu_A^i}{i!} \qquad \text{for } i = 0, 1, 2, 3,... \quad (19)$$

$$n_B^0(i) = N_{drop,B}\frac{e^{-\mu_B}\mu_B^i}{i!} \qquad \text{for } i = 0, 1, 2, 3,... \quad (20)$$

which after mixing equal volumes of these two microemulsions become

$$n_A(i;t=0) = \frac{1}{2}n_A^0(i) \qquad \text{for } i = 1, 2, 3... \quad (21)$$

$$n_B(i;t=0) = \frac{1}{2}n_B^0(i) \qquad \text{for } i = 1, 2, 3... \quad (22)$$

Table 4. Dependence of Time Scale of Formation of Bivariate Drops ($\bar{\tau}_b$) on Mean Number of Reactant Molecules Per Drop (μ)

μ	$\bar{\tau}_b$
0.1	$O(10^2)$
0.5	$O(10)$
1	$O(4)$
2	$O(1)$

The nondimensional number density of empty drops at time $t = 0$ is obtained as follows:

$$\bar{n}(0; t=0) = 1 - \sum_{i=1}^{\infty}\bar{n}_A(i;t=0) - \sum_{i=1}^{\infty}\bar{n}_B(i;t=0) \quad (23)$$

while for all the other classes of drops it is zero.

$$\bar{n}_k(i, j; t=0) = 0 \qquad \text{for } k = \text{CA, CB, SA, SB} \quad (24)$$

The average volume equivalent spherical diameter of particle population is calculated by

$$d_{av}(t) = \left[\frac{6i_{av}(t)M_W}{\pi\rho N_A}\right]^{1/3} \quad (25)$$

For the bivariate PBE model, i_{av} is calculated as follows.

$$i_{av}(t) = \frac{\sum_{i=n^*}^{Z_{max}}\sum_{j=0}^{Z_{max}} i\bar{n}_{SA}(i,j,t) + \sum_{i=n^*}^{Z_{max}}\sum_{j=1}^{Z_{max}} i\bar{n}_{SB}(i,j,t)}{\sum_{i=n^*}^{Z_{max}}\sum_{j=0}^{Z_{max}} \bar{n}_{SA}(i,j,t) + \sum_{i=n^*}^{Z_{max}}\sum_{j=1}^{Z_{max}} \bar{n}_{SB}(i,j,t)} \quad (26)$$

The set of coupled first-order ordinary differential eqs A1, A2, A3 and similar equations for $\bar{n}_B(i)$, $\bar{n}_{CB}(i,j)$, and $\bar{n}_{SB}(i,j)$ (as in Appendix A) are solved numerically by the Runge−Kutta method[41] using initial conditions from eqs 21−24, to obtain the mean aggregate number (MAN), which is also proportional to the mean particle size, and complete particle size distribution (PSD) from this model. The number of terms in any of the infinite summation series (of equations given in Appendices A and B) are truncated at some positive integer Z_{max}, such that further increase in Z_{max} does not change the result (e.g., MAN, PSD, etc.) to any significant extent. Typical values of Z_{max} used for different cases are 40−70.

In the univariate PBE model, i_{av} can be calculated in a simple way. It is possible to write n^{th} moment of number density ($\bar{n}_S$) in a closed form, which is

$$M_S^{(n)}(t) = \sum_{i=n^*}^{\infty} i^n\bar{n}_s(i,t) \qquad n = 0,1,2,3... \quad (27)$$

Zeroth and first moments of $\bar{n}_S$ (eqs B5 and B6) are derived from eqs B4 and 27. Equations B1−B3, B5, and B6 are then solved together as part of the univariate model. For initial conditions we use eqs 21−23, with zero for other population number densities and moments. Afterward, i_{av} is calculated from

(41) Gupta, S. K. *Numerical Methods for Engineers*; New Age International Ltd.: New Delhi, 1995.

Table 5. Parameters Used in the PBE Models and MC Simulation

variables	values[a]
d_{drop} ($R = 5$)	4.2×10^{-9} m
d_{drop} ($R = 32$)	15.2×10^{-9} m
k_0	278.42 s^{-1}
K_s	3.6×10^{-29} mol^2 L^{-2}
N	100 000
n^*	2
N_{drop} ($R = 5$)	1.084×10^{24} m^{-3}
N_{drop} ($R = 32$)	1.566×10^{23} m^{-3}
q_d	1.097×10^{-17} m^3 s^{-1}
T	298 K
v_m	5.24×10^{-29} m^3
β_d ($R = 5$, $x = 2, 5, 10$)	10^{-4}
β_d ($R = 32$, $x = 2$)	0.10
β_d ($R = 32$, $x = 10$)	0.01
η	0.001 kg m^{-1} s^{-1}
σ	0.1 N m^{-1}

[a] Values are taken from ref 27.

the ratio of first moment to zeroth moment of $\bar{n}_S$ as follows.

$$i_{av}(t) = \frac{M_S^{(1)}(t)}{M_S^{(0)}(t)} \tag{28}$$

Results and Discussion

4.1. Comparison of Bivariate Model Results with Experiments. Experiments of Lianos and Thomas[14] on the preparation of CdS nanoparticle by the method of two microemulsions are compared with the results of the PBE models of this paper and both previous[27] and new MC simulation results. These experimental data had been earlier simulated by Bandyopadhyaya et al.[27] using MC simulation with binomial redistribution, to which we have now added the results of MC simulation with cooperative redistribution, for assessing the role of redistribution. The PBE model formulation is consistent with MC simulation, except that the former is deterministic, while the latter is stochastic in nature. All the parameters and constants used in the model and simulation are given in Table 5.

In the experiments,[14] two water/AOT/heptane microemulsions, one containing cadmium perchlorate and the other containing sodium sulfide, are mixed to form CdS nanoparticles. Nanoparticle size was reported in terms of MAN of CdS nanoparticles, which is measured from emission quenching of CdS. Experiments were conducted for various molar ratios of water to surfactant (R) and molar ratios (x) of $[Cd^{2+}]$ to $[S^{2-}]$. Comparison of the final value [after 100% conversion to CdS nanoparticle] of MAN from experiment, bivariate PBE model, and MC simulation is shown in Figure 3a and 3b for $R = 5$ and $R = 32$, respectively. The mean number of reactant molecules per drop for these R and x values are shown in Table 6. Both the model and simulation results predict the same MAN (and hence same CdS particle size) for all R, x, and redistribution modes, establishing the close connection between PBE and MC, and validating both these approaches for predicting the nanoparticle synthesis mechanism. In addition, a reasonably good agreement with experiments is observed from both PBE and MC results when binomial redistribution is used (Figure 3). For example, in Figure 3a, for $x = 2$ and 10, both the PBE and MC results compare well with experiments, but for $x = 5$, there is some deviation. Furthermore, in Figure 3b, for both $x = 2$ and 10, there is excellent agreement between experiments with PBE and MC with binomial redistribution. Finally, both PBE and MC calculations very well reproduce the experimental trend of increasing MAN (and hence particle size) with an increase in R (i.e., drop size). This is clearly evident on comparing the increasing trend in MAN from Figure 3a to 3b.

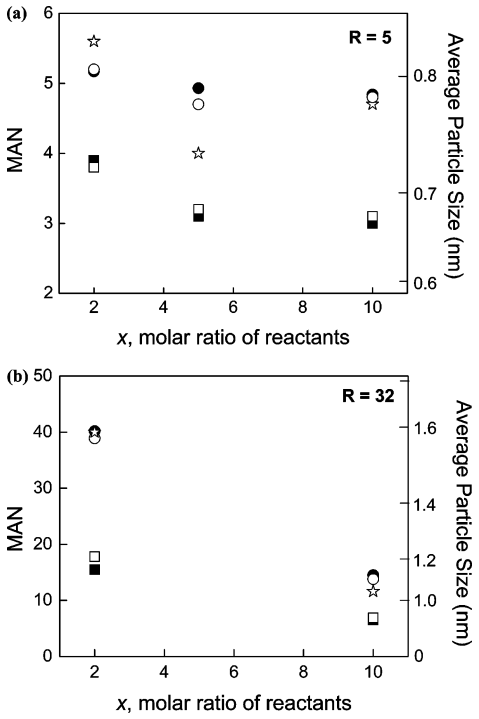

Figure 3. Comparison of the final mean aggregate number (MAN) from the bivariate PBE model and MC simulation with experiments. (☆) Experiment;[14] (●) PBE-binomial; (○) MC-binomial;[27] (■) PBE-cooperative; (□) MC-cooperative. Note that some data points exactly overlap each other.

Table 6. Mean Number of Reactant Molecules at Various R and x Values (Used in Experiments[14] and in Our Parametric Study)

R	x	$[Cd^{2+}]$, M	μ_{Cd}	$[S^{2-}]$, M	μ_S	remarks
5	1[a]	0.001	0.555	0.001	0.555	Figure 4a−4c
	1[a]	0.002	1.110	0.002	1.110	”
	1[b]	0.005	2.775	0.005	2.775	”
	1[b]	0.010	5.550	0.010	5.550	”
	2[a]	0.001	0.555	0.0005	0.2775	Figures 3a−3b and 6a−6b
	5[a]	0.0005	0.2775	0.0001	0.0555	”
	10[a]	0.001	0.555	0.0001	0.0555	”
32	2[a]	0.0002	0.7692	0.0001	0.3846	”
	10[b]	0.001	3.8460	0.0001	0.3846	”

[a] $\mu < n^*$. [b] $\mu > n^*$ since $n^* = 2$.

The redistribution mode of molecules is crucial in nanoparticle formation, because reaction, nucleation, and growth are all functions of the occupancy of reactant and product molecules in a drop, distributions of which among drops change continuously due to coalescence-exchange. The cooperative mode compared to binomial redistribution or experiments results in a very much underpredicted MAN (Figure 3a and 3b). This is because, in cooperative redistribution, reactant and product molecules are preferentially transferred to one of the drops after redispersion of the dimer. This leads to more drops having critical nuclei and an increased nucleation rate, making less C(l) molecules available for growth, given the same amount of total product. As a consequence, a greater number of particles with less MAN (or particle size) is obtained in the cooperative mode,

compared to the experimentally proven correct mode of binomial redistribution.

4.2. Effect of Reactant Concentration. The productivity of nanoparticles can be increased by increasing the initial concentration of reactants. However, reactant concentration also affects average nanoparticle size (d_{av}) and particle size distribution (PSD). Therefore, the questions that need to be answered are how reactant concentration affects d_{av} and PSD and in what range of concentrations is the effect more significant. For example, it may be of interest to synthesize a large quantity of nanoparticles without changing d_{av} and PSD. With this motivation, a range of concentrations is analyzed, and corresponding μ values are given in Table 6. The chosen reactant concentrations span the range $\mu < n^*$ to $\mu > n^*$, as shown in footnotes for Table 6.

The total mass of product increases proportionally with reactant concentration in Figure 4a to 4c. Figure 4a shows buildup of C(l) and N_p with time, for various Cd^{2+} concentrations, at $R = 5$ and $x = 1$. As the concentration is increased, a larger amount of C(l) is formed at a faster rate. However, since the nucleation rate increases with occupancy, the extra C(l) formed at short times for higher concentrations depletes equally faster into CdS nanoparticles. This is evident from the shape of C(l) curves, which are much more shallow at lower concentrations, due to both slower buildup of C(l) and slower nucleation over a longer period of time compared to C(l) curves at higher concentrations. Figure 4a also shows the expected increase in the final value of N_p with reactant concentration. N_p saturates at shorter times for higher concentrations, compared to that for lower concentrations. This is due to the same reason of increased nucleation rate in the former case.

As shown in Figure 4b, d_{av} also increases with reactant concentration. Therefore, we conclude from Figures 4a and 4b that the availability of more C(l) due to an increase in concentration increases both the extent of nucleation and growth by coalescence-exchange, and hence N_p and d_{av}, respectively. Nevertheless, when $\mu < n^*$, the effect is more pronounced on nucleation than growth, so as to increase N_p, rather than d_{av}. Hence, under this condition of $\mu < n^*$, the productivity of nanoparticles can be increased without any appreciable change in d_{av}. For higher concentrations ($\mu > n^*$), both N_p and d_{av} increase appreciably, which have generally been observed in experiments[12,16] and other modeling studies[21,25,42] also.

Since we solve for individual number densities in our bivariate PBE model, rather than only moments, we also obtain the PSD from the model (Figure 4c). At lower reactant concentrations ($\mu < n^*$), due to the nature of the Poisson distribution, the number density of drops having n^* or more number of C(l) molecules will be very low. Therefore, only a few drops can have a nucleus, while C(l) molecules present in other drops (those where the number of C(l) molecules is less than n^*) contribute to the growth of existing nuclei. The size distribution of nuclei will be narrow because most of them form with a size corresponding to n^* number of $C(l)$ molecules. In addition, the potential number of drops which can have a nucleus increases with reactant concentration. Therefore, when $\mu < n^*$, increasing concentration favors a larger number of nearly equal sized nuclei, so that the PSD does not change (first two curves in Figure 4c). In contrast, for higher reactant concentrations ($\mu > n^*$), the number density of drops having n^* or more number of C(l) molecules is much more, resulting in a wider distribution in nuclei size. Previous time-scale analysis (section 3.1) shows that nucleation and nanoparticle growth by coalescence-exchange of drops are competitive processes. Hence, the availability of more C(l) molecules (by way of increased reactant concentration) in this case is used for both nucleation and growth. Therefore, when $\mu > n^*$, increased reactant concentration results in a wider PSD (last two curves in Figure 4c) because of these two combined effects. The latter trend has also been reported by others from their experiment[12] and PBE models.[21,25]

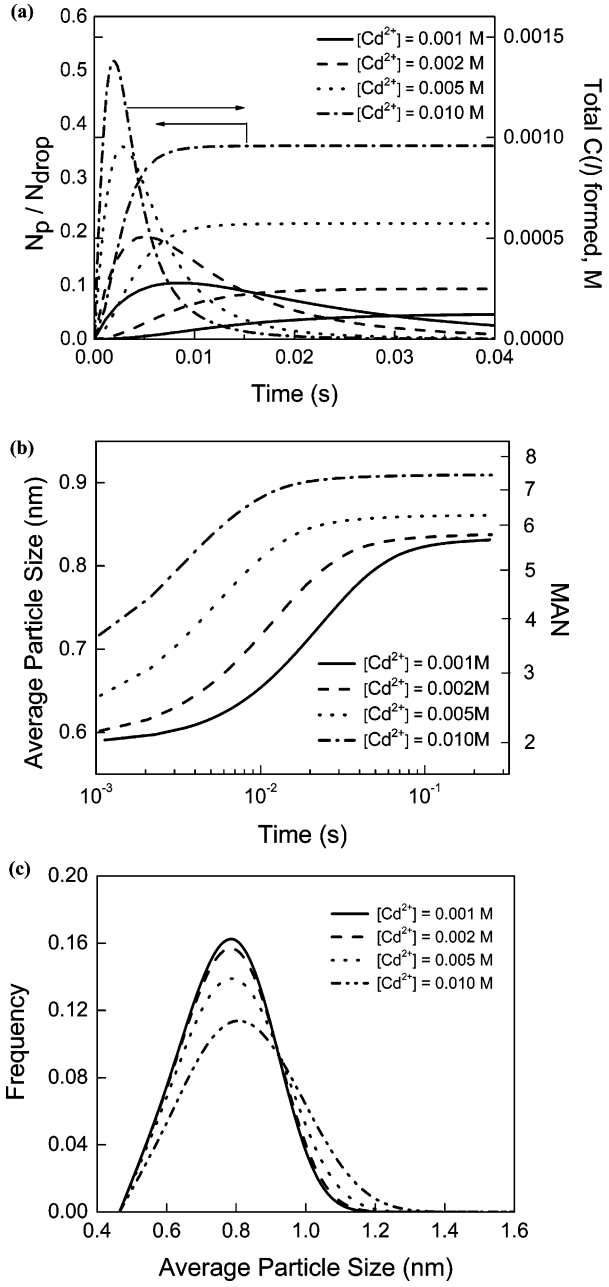

Figure 4. Effect of reactant concentration on (a) temporal evolution of number of nanoparticles formed and buildup of C(l), (b) temporal evolution of average particle size, and (c) final particle size distribution (PSD) at $R = 5$ and $x = 1$, from the bivariate PBE model with binomial redistribution.

4.3. Effect of Molar Ratio of Reactants. Lianos and Thomas reported[14] that if CdS nanoparticles are synthesized with excess cadmium ions, the emission property of CdS gets enhanced.

(42) Tojo, C.; Blanco, M. C.; Lopez-Quintela, M. A. *Langmuir* **1997**, *13*, 4527.

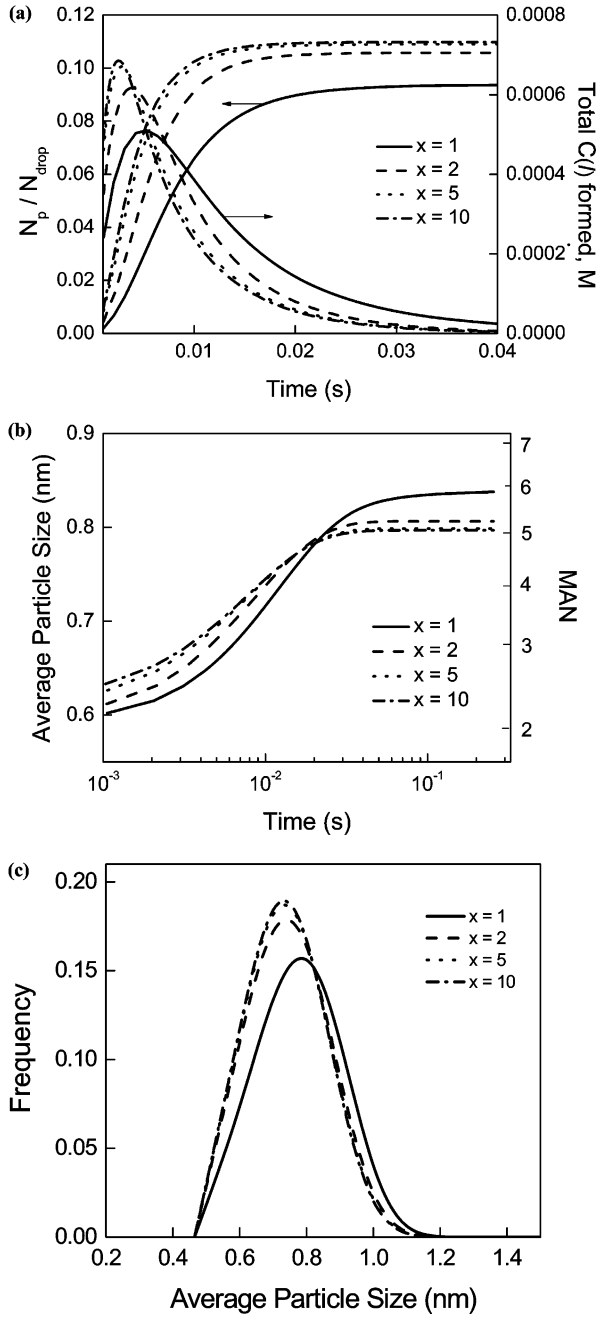

Figure 5. Effect of molar ratio of reactants on (a) temporal evolution of number of nanoparticles formed and buildup of C(l), (b) temporal evolution of average particle size, and (c) final particle size distribution (PSD) at $R = 5$ and $[S^{2-}] = 0.002$ M, from the bivariate PBE model with binomial redistribution.

This finding is technologically important because improved photoemission is desired for device fabrication. On the other hand, synthesizing nanoparticles with an excess of one of the reactants affects d_{av}, which itself causes variation in photoemission. Now excess reactant affects the rate of formation of C(l) and hence the nucleation rate and d_{av}. It is, therefore, essential to understand the role of an excess reactant on d_{av}. At $R = 5$, for a fixed $[S^{2-}]$ concentration of $C = 0.002$ M, the effect of varying x in the experimental range from 1 to 10 is shown in Figure 5a−5c. In comparing these cases, we need to remember that the relative rates of formation and loss of C(l) via coalescence-exchange and nucleation varies; however there is no change in the total mass of CdS particles formed. At higher

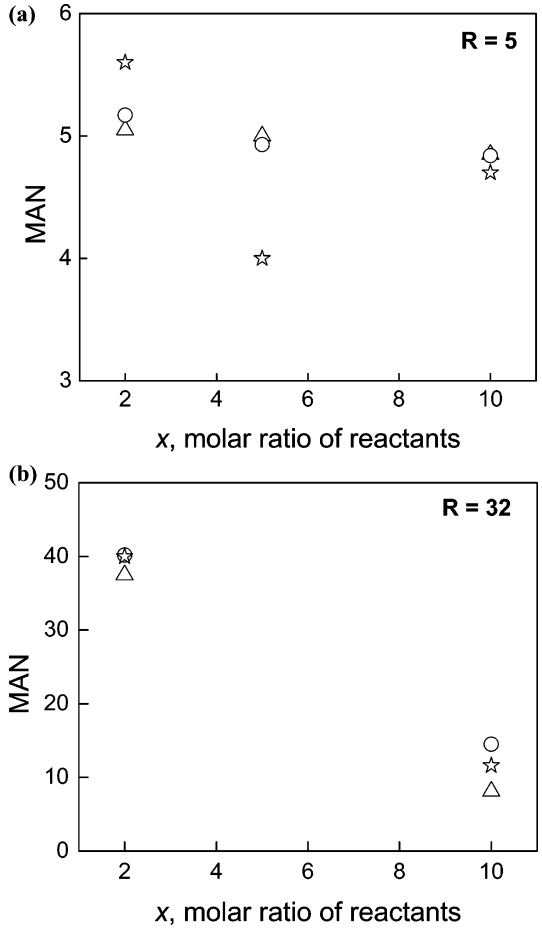

Figure 6. Comparison of the final mean aggregate number (MAN) from bivariate and univariate PBE models (binomial mode) with experiments. (★) Experiment;[14] (○) Bivariate PBE; (△) Univariate PBE. Note that some data points exactly overlap each other.

x, buildup of C(l) is faster leading to a higher nucleation rate. Hence, N_p increases with x (Figure 5a) up to $x = 5$, after which further increases in x have no additional effect.

Figure 5b shows the evolution of particle size (d_{av}) as a function of time under the same conditions but with different amounts of excess reactant. Since the nucleation rate is enhanced at higher x, d_{av} decreases with x as the total amount of product CdS is constant. However, this effect is insignificant beyond $x = 5$, and the average particle size does not change anymore. It is known that physicochemical properties (photoemission) of nanoparticles depend on both d_{av} and x. Lianos and Thomas[14] has shown that the intensity of emission spectra increases continuously from $x = 2$ to 10. However, from Figure 5b we know that d_{av} does not change beyond $x = 5$. Therefore, further increase in photoemission observed by those authors is due to adsorption of the excess Cd^{2+} ion on the surface of the CdS nanoparticle. Our model hence clearly brings out the role and extent of excess reactant to be used, for a beneficial increase in emission intensity of CdS. Furthermore, Figure 5c shows that when x is increased from 1 to 5, the final size distribution of CdS nanoparticles shifts slightly toward smaller sizes, concomitant to the decrease in d_{av} (Figure 5b), but no apparent change in width of the distribution. Finally, there is no further change in either d_{av} or PSD for $x > 5$ (Figure 5c).

4.4. Comparison of Univariate and Bivariate Model Results with Experiments. In Figure 6a and 6b, results of the

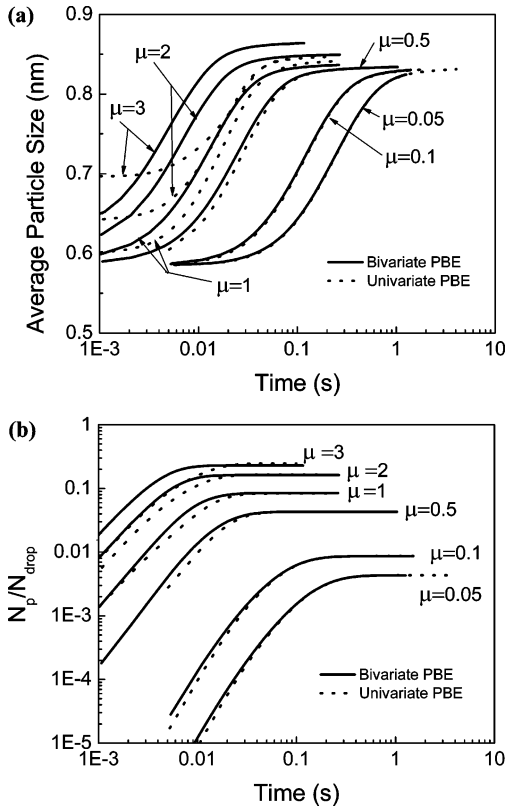

Figure 7. Comparison of bivariate and univariate PBE models (binomial mode) for various mean numbers of reactant molecules (μ) at $R = 5$ and $x = 1$. (a) Evolution of average particle size with time. (b) Evolution of number of nanoparticles with time.

univariate PBE model are compared with those of the bivariate PBE model and experiments.[14] Results of both the models compare nearly exactly with each other at all x values for $R = 5$ but only at $x = 2$ for $R = 32$. However, at $x = 10$ for $R = 32$, there is clearly some deviation (Figure 6b). Therefore, our simplifications in deriving the univariate model do not introduce any significant error in the prediction of the final MAN (i.e., particle size) in a certain range of synthesis conditions. For example, for $R = 32$ and $x = 10$, $\mu_A = 3.846$ and $\mu_B = 0.3846$. In such cases, the assumptions of pseudo steady state approximation for bivariate populations are not correct. Therefore, the bivariate populations that are neglected in the univariate model may be significant.

To establish the range of applicability of the univariate PBE model, results from it are compared with those of the bivariate model for various μ values (ranging from 0.05 to 3), at $R = 5$ and $x = 1$ (Figure 7a and 7b). In the range $\mu = 0.05$ to 0.5, both model predictions agree nearly exactly to each other, not only with respect to final values of d_{av} and N_p but also in their temporal evolution. For $\mu = 1$, the final particle size of both the models match (Figure 7a) but a maximum error of 5% in the evolution of d_{av} is observed. However, for $\mu > 1$, this error in temporal evolution of d_{av} becomes progressively more, although final particle size still compares very well with that from the bivariate model, within an error of 1% only. Similarly, for all μ values studied, the final N_p predicted from the univariate model matches exactly with that from the bivariate model. However, for $\mu > 1$, the univariate model compared to the bivariate model shows a delayed nucleation, causing a difference in temporal evolution of N_p, and hence that of d_{av} too. Therefore, the univariate model can be used when both μ_A and $\mu_B \leq 1$. The successful prediction of experimental data for all x values at $R = 5$ (Figure 6a) is attributed to the fact that $\mu < 1$ in these cases, for both the reactants.

So the bivariate PBE model predicts experimental data quite reasonably for a wide range of R and x values, while the univariate PBE model predicts final values very well for all cases, but the temporal evolution, only when $\mu < 1$ for both reactants. However, the number of equations to be solved in the univariate model is reduced to $\sim 3Z_{max}$ from $\sim 2Z^2_{max}$ equations of bivariate model. This is because there are only univariate populations, with bivariate drops and consequently their number density equations being eliminated. This step also simplifies the remaining equations (compare eqs A1 with B1, A2 with B3, and A3 with B4), as a large number of terms in the bivariate PBEs drop out. Furthermore, with Z_{max} in the range of 40 to 70, this is a reduction in the number of equations by nearly two orders of magnitude. Both these facts together led to a reduction in computational time from 6 to 8 h for the bivariate model to less than a minute for the univariate model, in a computer with a 3.4 GHz Pentium IV processor. Although the univariate model does not provide the complete PSD, as in the bivariate version, the standard deviation of the PSD can be calculated in the former by solving higher order moments of $\bar{n}_S$.

5. Conclusions

A deterministic bivariate population balance equation (PBE) based model has been formulated to predict the nanoparticle size distribution synthesized by mixing two reactive w/o microemulsion solutions. Both the solutions contain predissolved reactants. Therefore, nanoparticle formation in this self-assembled, confined system involves coalescence-exchange of water drops and reaction of drop contents, followed by nucleation and growth of nanoparticles within the drop. Time scales calculated based on the rates of these elementary events show that reaction and growth are instantaneous, compared to coalescence-exchange and nucleation. We have implemented for the first time in such a model the correct mechanism of binomial redistribution of molecules after collision between water drops, which is shown to have a significant impact on model predictions. Experimental data[14] on the mean aggregate number (MAN) and hence the size of CdS nanoparticles, under various synthesis conditions, like different molar ratios of reactants (x) and molar ratios of water to surfactant (R) are predicted reasonably well by the bivariate PBE model. The model results are also in excellent agreement with those of previously published[27] and new Monte Carlo (MC) simulations carried out in this work, predicting experimental CdS synthesis data.[14]

The importance of the mode of redistribution of molecules on nanoparticle formation is also elucidated in the present work. The cooperative redistribution mechanism (used previously[25]) underpredicts experimental particle size (or MAN), while the binomial redistribution mode used in this work shows a good comparison with experiments. This highlights the need to account for the correct redistribution mechanism in nanoparticle formation.

(43) Rosner, D. E.; Pyykonen, J. J. *AICHE J.* **2002**, *48*, 476.

Model calculations showed that for a low reactant concentration ($\mu < n^*$), with a stoichiometric reactant ratio ($x = 1$), the final mean CdS particle size does not change appreciably on increasing μ. However, the number of particles formed increases proportionally with reactant concentration. Therefore the production rate of nanoparticles can be increased without affecting final particle size. In contrast, for higher concentrations ($\mu > n^*$), both CdS particle size and number of particles increase, while particle size distribution (PSD) broadens out, with a tail in the PSD at higher sizes. These trends captured by our model are validated by other experiments,[12,16] lending further credence to the generality of our model. It is known that excess Cd^{2+} ion can adsorb on CdS nanoparticle surface during synthesis and cause a favorable enhancement in emission intensity. Therefore, to assess the role of using an excess of Cd^{2+} ion, we fixed the concentration of the limiting reactant [S^{2-}] at 0.002 M and increased x from 1 to 10. From $x = 1$ to 5, the final mean CdS particle size decreases, with a concomitant increase in the number of particles, implying an enhanced nucleation compared to growth. A further increase from $x = 5$ to 10 has no additional effect on the number, mean size, or final particle size distribution of CdS. So the experimentally observed increase in emission intensity of CdS for $x > 5$ is purely due to surface adsorption of excess Cd^{2+} ions, and not due to any particle size induced effect.[14] Thus, the present work shows how to tune experimental conditions to produce CdS nanoparticles of desired size. This, when combined with previous molecular simulation studies of correlating CdS cluster or nanoparticle structure with properties,[5] can provide a powerful tool for designing specific CdS nanomaterials.

A computationally efficient univariate PBE model employing a set of univariate drops has also been developed. It is derived by making a pseudo steady state approximation in the bivariate model. Time-scale analysis offers a good a priori choice of the appropriate model (based on range of μ for both the reactants) for the nanoparticle synthesis process at hand. Indeed, for the CdS case studies discussed in this paper, we find that the univariate model is very well applicable when $\mu < 1$; and maybe even up to $\mu = 1$ with only a small deviation from the complete bivariate model. Under the condition $\mu < 1$ for both the reactants, the univariate model yields very good predictions for both temporal evolution and final particle characteristics.

The univariate model has several advantages over the bivariate model. First, for $\mu < 1$, the bivariate model need not be used, eliminating many classes of drops from our consideration. Second, the univariate model can be solved using moment transformation, instead of solving for individual number densities [like, $\bar{n}_{SA}(i,j)$ and $\bar{n}_{SB}(i,j)$], thus reducing computation time significantly. For modeling continuous flow processes involving nanoparticle formation, PBE models are coupled to the transport equations of mass, momentum, and energy balance.[43] A univariate PBE model will be desirable in these cases to perform a rapid assessment of the flow reactor performance and quality of the nanoparticulate product obtained thereof. Although the univariate model will not provide complete PSD like the bivariate model, the standard deviation can still be calculated in the former by solving higher order moments of $\bar{n}_S$.

Acknowledgment. The authors thank Mr. Kanchan Dutta, IIT Kanpur, for performing MC simulations with cooperative redistribution.

Supporting Information Available: PBE equations for both bivariate (Appendix A) and univariate (Appendix B) models of nanoparticle formation, a complete list of nomenclature for symbols used (Appendix C), and complete ref 3. This material is available free of charge via the Internet at http://pubs.acs.org.

JA0652621